

Anisotropic Thermal Conductivity of Pyrolytic Graphite

GLEN A. SLACK

General Electric Research Laboratory, Schenectady, New York

(Received March 21, 1962)

The thermal conductivity K of a bulk sample of pyrolytic graphite has been measured from 3 to 300°K both perpendicular and parallel to the c axis. Over the whole temperature range below 100°K the thermal conductivity in both directions appears to be limited by the crystallite size. The measured value of K_{\perp} is 0.72 W/cm deg at 300°K, and K_{\perp} decreases monotonically to 1.4×10^{-4} W/cm deg at 3°K. The measured anisotropy K_{\perp}/K_{\parallel} decreases monotonically from 47 at 300°K to 2.5 at 3°K. A theoretical calculation of the anisotropy from the elastic constants yields a value of 2.27 for $T \leq 1^{\circ}\text{K}$. A suggestion is offered to explain the rapid rise in the anisotropy with increasing temperature. Previous measurements of K_{\perp}/K_{\parallel} in natural and commercial graphite samples are much smaller.

INTRODUCTION

GRAPHITE has an hexagonal crystal structure and has been known for a long time as an anisotropic material.¹ This anisotropy has become important with the recently renewed interest in well-oriented samples of pyrolytic graphite.^{2,3} Many of its physical properties, including its thermal conductivity K , are anisotropic. The present paper reports some recent measurements of the anisotropy in K , reviews some of the previous measurements of K on various graphites, and presents a theoretical calculation of the anisotropy of K for $T \leq 1^{\circ}\text{K}$.

Most of the commercial products commonly called carbons and graphites are very poorly oriented agglomerations of carbon atoms in both aromatic (planar) and tetrahedral (diamond-type) bonding.^{4,5} Their thermal conductivities both above and below room temperature have been reviewed by various authors.⁶⁻⁸ Values of K for these materials at 300°K range from about 0.02 to 4 W/cm deg. The main conclusion of this early work is that K depends on the size of the graphite crystallites, the perfection of the individual crystallites, the fraction of nongraphitic carbon present between the crystallites, and slightly on the orientation of the crystallites.

Our present interest is in graphite which possesses a high degree of perfection in its crystallite size and orientation, and possesses very little nongraphitic carbon. Pyrolytic graphite is a step in this direction.⁹ The K results on natural and commercial graphite specimens are also of interest. Table I lists most of the available data in the literature¹⁰⁻¹⁴ on the K of natural

graphite (NG) specimens at 300°K. The values given in Table I are for K_{\perp} the thermal conductivity, and σ_{\perp} the electrical conductivity, measured in a direction perpendicular to the c axis of the majority of the graphite crystallites. When available, the anisotropy ratios K_{\perp}/K_{\parallel} and $\sigma_{\perp}/\sigma_{\parallel}$ are given. Both of these ratios are greater than unity. The K_{\perp}/K_{\parallel} ratio for the NG samples varies from 3 to 6, thus indicating the thermal as well as the electrical conductivity is greater along the tightly bound graphite planes than across them where the binding is weak. In highly perfect graphite the carbon-carbon atom distance in the planes is 1.415 Å, while the interplanar spacing is 3.35 Å.

Similar anisotropic behavior is evident in artificially produced commercial graphites (CG). For example, extruded samples have been measured by Powell¹⁵ and by Buerschaper.¹⁶ These samples gave K_{\perp}/K_{\parallel} ratios at 300°K of 1.15 and 1.6, respectively.

The K_{\perp} and σ_{\perp} values shown in Table I for the pyrolytic graphite (PG) specimens^{6,17-22} are of the same order of magnitude as for the natural graphites and the commercial graphites. However, because of the highly preferred orientation of the crystallites in pyrolytic graphite, the anisotropies K_{\perp}/K_{\parallel} and $\sigma_{\perp}/\sigma_{\parallel}$ are much greater. The data available in the present literature^{17,18,21} indicate K_{\perp}/K_{\parallel} ratios for pyrolytic graphite from 95 to 500 at 300°K, and even higher $\sigma_{\perp}/\sigma_{\parallel}$ ratios.

¹¹ R. W. Powell, *General Discussion on Heat Transfer* (Institute of Mechanical Engineers, London, 1951), p. 290.

¹² J. Koenigsberger and J. Weiss, *Ann. Physik* **35**, 1 (1911).

¹³ E. Jannettaz, *Bull. soc. min. France* **15**, 133 (1892).

¹⁴ A. W. Smith, *Phys. Rev.* **95**, 1095 (1954).

¹⁵ See reference 8, samples 21 and 22.

¹⁶ R. A. Buerschaper, *J. Appl. Phys.* **15**, 452 (1954).

¹⁷ Raytheon Company, *Electronics*, **32**, 124 (1959).

¹⁸ E. F. Keon, Fourth Biennial Conference on Carbon, University of Buffalo, June 15, 1959, (unpublished), Paper No. 74; also *Pyrographite*, High Temperature Materials Department, (Raytheon Company, Waltham, Massachusetts, 1959).

¹⁹ A. R. G. Brown, W. Watt, R. W. Powell, and R. P. Tye, *Brit. J. Appl. Phys.* **7**, 73 (1956); see also reference 7.

²⁰ M. Pirani and W. Fehse, *Z. Elektrochem.* **29**, 168 (1923).

²¹ Raytheon Company, *Sci. American*, **201**, 105 (1959); *Chem. and Eng. News* **37**, 56 (1959). See also *Note added in proof*.

²² J. C. Bowman, J. A. Krumhansl, and J. T. Meers, *Industrial Carbon and Graphite* (Society of Chemical Industry, London, 1958), p. 52.

¹ A. R. Ubbelohde and F. A. Lewis, *Graphite and Its Crystal Compounds* (Oxford University Press, Oxford, 1960).

² W. E. Sawyer, U. S. Patent No. 229,335 (1880).

³ A. R. G. Brown, A. R. Hall, and W. Watt, *Nature* **172**, 1145 (1953); C. A. Klein, *Revs. Modern Phys.* **34**, 56 (1962).

⁴ J. Kakinoki, K. Katuda, T. Hanawa, and T. Ino, *Acta Cryst.* **13**, 171 (1960).

⁵ A. W. Smith, *Phys. Rev.* **93**, 952 (1954).

⁶ A. W. Smith and N. S. Rasor, *Phys. Rev.* **104**, 885 (1956).

⁷ R. Berman, *Industrial Carbon and Graphite* (Society of Chemical Industry, London, 1958), p. 42.

⁸ R. W. Powell, *Industrial Carbon and Graphite* (Society of Chemical Industry, London, 1958), p. 46.

⁹ C. A. Klein and W. D. Straub, *Phys. Rev.* **123**, 1581 (1961).

¹⁰ R. Berman, *Proc. Phys. Soc. (London)* **A65**, 1029 (1952).

TABLE I. Thermal and electrical conductivities and anisotropies of graphite samples at 300°K.

Sample number	Source	ρ (g/cm ³)	K_1 (W/cm deg)	σ_1 (10 ³ Ω ⁻¹ cm ⁻¹)	K_1/K_{11}	σ_1/σ_{11}	Reference
NG-10	Ceylon ^b	2.17	2.4	1.02	3.2	4.2	10
NG-11	Cumberland	2.21	3.1	1.42	~6	~9	11
NG-12	Ceylon	~2.2	3.6	2.8	12
NG-13	Ceylon ^b	2.17	4.2	2.9	4.8	6.7	11
NG-14	natural	~2.2	6.2	...	13
NG-15	Canada	~2.25	4.5	7.7	14
CG-16	G.L.C.C.	~1.7	1.3	1.07	1.15	1.20	15
CG-17	N.C.C.	~1.6	1.7	1.60	1.6	2.3	16
PG-0	G.E.C.	2.19	0.72	1.85	46	930	^c
PG-18	N.C.C.	~2.2	1.1	3.3	6
PG-19	R.C.	~2.1	~2.7	4.4	~95	1000	17
PG-20	R.C.	2.17	4.1	4.4	110	1000	18
PG-21	R.A.E.	2.15	5.8	4.1	19
PG-22	O.K.	~2.15	>4	~11	20
PG-23	R.C.	500	1000	21
PG-24	N.C.C.	~2.25	21	14	22
Single crystal		2.265	~20	25	1000(?)	~2×10 ⁴	see text

^a CG = Commercial graphite, NG = natural graphite, PG = pyrolytic graphite, G.E.C. = General Electric Co., G.L.C.C. = Great Lakes Carbon Corp., N.C.C. = National Carbon Co., O.K. = Osram Konzern, R.A.E. = Royal Aircraft Establishment, and R.C. = Raytheon Company.

^b both from same block of Ceylon graphite (reference 8).

^c present data

PRESENT EXPERIMENT

The present experiment, performed on a pyrolytic graphite sample, was designed to measure both K_1 and K_{11} over the temperature range from 3 to 300° K by a technique previously employed.²³ It was hoped that the results would tell whether the anisotropies K_1/K_{11} , of the natural graphites (NG) or the pyrolytic graphites (PG), as given in Table I, are more nearly characteristic of well-ordered graphite. The K_1/K_{11} anisotropies reported^{17,18,21} for pyrolytic graphite are much larger than for any other material known. Some of the largest previous values reported,²⁴ all on natural minerals, are those for mica-6, brucite [Mg(OH)₂]-7, slate-8, and slaty-talc-9. Only nonmetallic materials are considered in the present paper. The anisotropy in K of some metals and semiconductor crystals can be as large^{13,23,25} as 5. As can be seen from Table I, the present measurements give $K_1/K_{11}=46$, $\sigma_1/\sigma_{11}=930$ at 300°K. These values agree with the earlier results of other authors on pyrolytic graphite, and indicate that the natural and commercial graphite samples in Table I are, really, nearly isotropic.

SAMPLE

The present sample (No. 271B, or PG-0 in Table I) of pyrolytic graphite was deposited²⁶ on a substrate of commercial graphite at 2250°C from a methane atmosphere at a total pressure of 20 mm Hg. Its measured density is 2.194 g/cm³. From x-ray measurements the graphite crystallites are thought to be shaped like oblate ellipsoids with rotational symmetry about the c axis. The minor diameter is $d_{11}=140$ Å and is parallel

to the c axis, the major diameter is $d_1=280$ Å and lies in the a - b plane. Macroscopically the sample is composed of columnar bundles of graphite of a maximum diameter of 0.1 cm. The average angular tilt of the crystallites in these columns away from the preferred c -axis orientation is 22°. Electrical conductivity measurements at 298°K give $\sigma_1=1.85\times10^3$ Ω⁻¹ cm⁻¹, $\sigma_{11}=1.98$ Ω⁻¹ cm⁻¹, and hence $\sigma_1/\sigma_{11}=930$. Sound velocity measurements²⁷ for longitudinal waves at 9.8 Mc/sec and 300°K give $v_1=4.7\times10^5$ cm/sec, $v_{11}=3.4\times10^5$ cm/sec for a ratio $v_1/v_{11}=1.4$. The average velocity, $\frac{1}{3}(2v_1+v_{11})=4.3\times10^5$ cm/sec, is in fair agreement with a value of 4.0×10^5 cm/sec of Wobschall and Hammill²⁸ on carbon rods. Their results have been linearly extrapolated to a theoretical density of 2.26 g/cm³.

The actual pieces, whose K was measured, were in the shape of solid rods of square cross section cut with the appropriate orientation. The K_1 sample was 1.9 cm long with a cross-sectional area of 0.14 cm². The K_{11} sample was 0.7 cm long and had an area of 0.17 cm². They were sound and free from any visible cracks along the (0001) planes. Both pieces were from the same large block of pyrolytic graphite, and came from the same region of the block.

RESULTS

In Fig. 1 the results of the K_1 and K_{11} measurements for the present sample of pyrolytic graphite PG-0 are shown over the temperature range 3 to 300°K. It is quite evident that $K_1>K_{11}$ over the whole temperature range, and that the anisotropy ratio K_1/K_{11} is a function of temperature. The present K_1 and K_{11}

²³ G. A. Slack, Phys. Rev. **122**, 1451 (1961).

²⁴ K. Schulz, Fortschr. Mineral Krist. Petrog. **9**, 221 (1924).

²⁵ R. W. Powell, Proc. Roy. Soc. (London) **A209**, 525 (1951).

²⁶ R. J. Diefendorf, J. chim. phys. **57**, 815 (1960).

²⁷ Courtesy of B. W. Roberts of this Laboratory.

²⁸ D. Wobschall and H. Hammill, *Fourth Conference on Carbon*, (Pergamon Press, New York, 1960), p. 577.

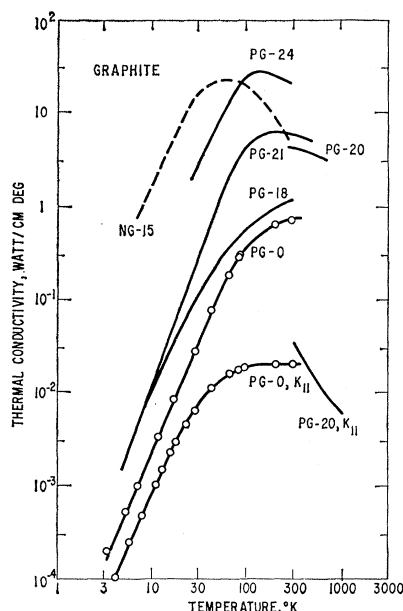


FIG. 1. The thermal conductivity K_{\perp} (perpendicular to the c axis) of various samples of pyrolytic graphite (PG) and one sample of natural graphite (NG). The values of K_{\parallel} (parallel to the c axis) are also shown for two of the PG samples.

values fall within the range of K values that have been measured for artificial carbons and graphite (not including pyrolytic graphite) at 300°K, i.e., 0.02 W/cm deg to 4 W/cm deg according to Powell.⁸ Other results from the literature for pyrolytic graphite^{6,18,19,22} and for a good single flake of natural graphite¹⁴ are also plotted. The values of K in Fig. 1 at 10°K vary over a range of 10^3 . This reflects the wide range of crystallite sizes in the samples studied.

The temperature dependence of K at low temperatures has been widely discussed in the past.^{5,6,14,29,30} For NG-15, PG-18, and PG-24 the value of K_{\perp} is proportional to T^2 . For PG-21, measured by Berman, $K_{\perp} \propto T^{2.8}$. For the present sample PG-0 it was found that $K_{\perp} \propto T^{2.4}$ and $K_{\parallel} \propto T^{2.3}$ for $T < 20^\circ\text{K}$. It does not appear to be true, as Smith and Razor⁶ have suggested, that pyrolytic graphite, *per se*, has a $K \propto T^2$ at low temperatures. The T^2 dependence may only hold for well-oriented and well-annealed pyrolytic graphite samples, such as PG-24 in particular. Furthermore, a $K \propto T^2$ dependence can only be valid over a limited range of temperatures since at very low temperatures ($T \leq 1^\circ\text{K}$) the specific heat capacity C will vary³¹⁻³⁵ as T^3 . Thus, since the phonon mean free path l should be

constant in this range, K should also vary as T^3 at sufficiently low temperatures. These temperatures will be at and below about 1°K according to Komatsu.^{32,33}

SIMPLE ANALYSIS OF THE RESULTS

As a first step, a simple analysis of the thermal conductivity results can be made. A more thorough analysis is introduced later. It is assumed that phonons are by far the dominant carriers of thermal energy in graphite. This has been rediscovered several times^{6,12,36} since 1897. Furthermore, the electrons do not affect the mean free path of the phonons.²² Therefore, only phonons enter the present discussion of K . At the lowest temperature of 3°K we can compute the phonon mean free path in the graphite planes l_1 from

$$l_1 = 3K_{\perp}/v_1C_T.$$

The numerical values are $K_{\perp} = 1.4 \times 10^{-4}$ W/cm deg, $v_1 = 4.7 \times 10^5$ cm/sec (measured), and $C_T = 1.3 \times 10^{-4}$ J/cm³ deg. Here C_T is the total heat capacity of the lattice for large crystallite size natural graphite.³⁷ The result is $l_1 \sim 700$ Å, which is to be compared to the x-ray value of 280 Å for d_1 . This agreement is not terribly bad, but it indicates that $l_1 > d_1$. Later it will be shown that $l_1 \approx 10d_1$.

An approximation to the anisotropy can be calculated from

$$K_{\perp}/K_{\parallel} = l_1v_1C_T/l_{\parallel}v_{\parallel}C_T. \quad (1)$$

Using the measured values of d and v , and assuming that $(l_1/l_{\parallel}) = (d_1/d_{\parallel})$, the computed anisotropy is 2.8 at 3°K. The measured value of K_{\perp}/K_{\parallel} at 3°K is 2.5. This is about as far as the simple analysis can be pushed.

A MORE RIGOROUS ANALYSIS

A detailed knowledge of the lattice vibrational modes of graphite and their dependence on temperature is required in order to understand the magnitude, temperature dependence, and anisotropy of K . Such an analysis has been carried out in some detail by various authors^{33,38} for the total specific heat capacity C_T as a function of temperature. Let us now restrict the discussion of the thermal conductivity of graphite to the temperature range $T \leq 1^\circ\text{K}$. In this temperature range the five elastic constants (c_{11} , c_{12} , c_{13} , c_{33} , c_{44}) are sufficient to describe the modes of vibration. The bending modes of the single graphite sheets, described by Komatsu and Nagamiya³¹⁻³³ by the elastic constant κ , are not important in this temperature range. The description of the normal modes at low temperatures has been given in detail by Komatsu.³² The normal modes can be considered, to a reasonable approximation,

²⁹ P. G. Klemens, Australian J. Phys. **6**, 405 (1953).

³⁰ J. E. Hove and A. W. Smith, Phys. Rev. **104**, 892 (1956).

³¹ K. Komatsu and T. Nagamiya, J. Phys. Soc. Japan **6**, 438 (1951).

³² K. Komatsu, J. Phys. Soc. Japan **10**, 346 (1955).

³³ K. Komatsu, J. Phys. Chem. Solids **6**, 380 (1958).

³⁴ J. A. Krumhansl and H. Brooks, J. Chem. Phys. **21**, 1663 (1953).

³⁵ J. C. Bowman and J. A. Krumhansl, J. Phys. Chem. Solids **6**, 367 (1958).

³⁶ L. Cellier, Ann. Physik **61**, 511 (1897).

³⁷ W. De Sorbo and G. E. Nichols, J. Phys. Chem. Solids **6**, 352 (1958).

³⁸ A. Yoshimori and Y. Kitano, J. Phys. Soc. Japan **11**, 352 (1956).

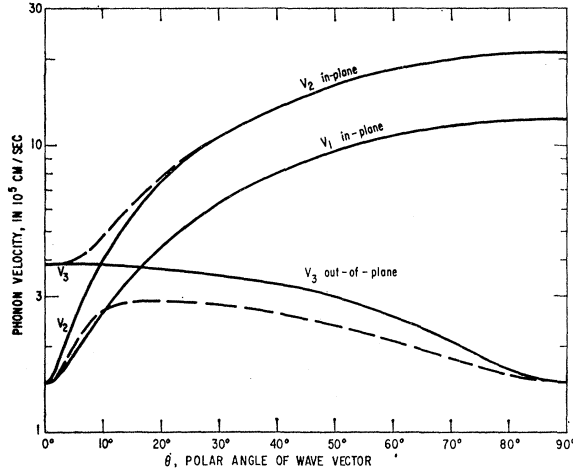


FIG. 2. The velocities v_1 , v_2 , v_3 of the three phonon branches as a function of the polar angle θ . These velocities are for the temperature range $T \leq 1^\circ\text{K}$. The dashed curves between v_2 and v_3 indicate the splitting of these two branches produced by c_{33} and c_{44} . This splitting is neglected in the present calculations.

to belong to three separate frequency branches ν_{10} , ν_{20} , ν_{30} [see Komatsu,³² Eq. (9)–(11)]. The propagation velocities v of these branches in low-temperature, long-phonon wavelength limit are

$$\begin{aligned} v_1^2 &= \rho^{-1}(c_{66} \sin^2\theta + c_{44} \cos^2\theta), \\ v_2^2 &= \rho^{-1}(c_{11} \sin^2\theta + c_{44} \cos^2\theta), \\ v_3^2 &= \rho^{-1}(c_{44} \sin^2\theta + c_{33} \cos^2\theta), \end{aligned} \quad (2)$$

where ρ is the crystal density, $c_{66} = (c_{11} - c_{12})/2$, and θ is the polar angle between the propagation vector σ and the c axis of the graphite crystal. Note that $|\sigma| = \lambda^{-1}$, where λ is the phonon wavelength. Figure 2 shows v_1 , v_2 , and v_3 as a function of θ using $\rho = 2.265 \text{ g/cm}^3$.

Since graphite has an hexagonal crystal structure, the velocities in Eq. (2) are independent of the azimuthal angle ϕ . The notation here is related to that of Komatsu^{31–33} by the equalities $c_{11} = \rho v_1^2$, $c_{66} = \rho v_2^2$, $c_{44} = \rho \zeta$, $c_{33} = \rho(\mu c)^2$.

The vibration characterized by ν_{10} and ν_1 is a purely transverse branch in which the atomic displacements lie within the graphite sheets. The ν_{20} , v_2 and ν_{30} , v_3 vibrations are, in the strict sense, both mixtures of two other strictly separated branches. This point is discussed later. For the present purposes no significant error is made if the ν_{20} and ν_{30} are considered as distinct and separate branches. Then the atomic displacements for the ν_{20} branch lie nearly in the plane of the graphite sheets for most values of θ . By contrast, the displacements for the ν_{30} branch lie nearly along the c axis for most values of θ . The ν_{10} and ν_{20} branches are called the “in-plane” vibrations, while ν_{30} is called the “out-of-plane” vibration. It will be seen later that the “out-of-plane” vibrations make the largest contribution to both K_L and K_{11} at low temperatures.

SPECIFIC HEAT CAPACITY

The specific heat capacity for $T \leq 1^\circ\text{K}$ can be calculated from these three pseudobranches with good precision. Let $S(\sigma, j)$ be the heat capacity of a particular normal mode of wave vector σ , polarization j , and frequency ν . The values of j are 1, 2, 3. Once σ and j are specified, then ν is determined. S , in terms of ν , is

$$S(\sigma, j) = k \left(\frac{h\nu}{kT} \right)^2 \frac{e^{h\nu/kT}}{(e^{h\nu/kT} - 1)^2}, \quad (3)$$

where k is Boltzmann's constant, h is Planck's constant, and T is the absolute temperature. The total heat capacity per unit volume C , of a crystal of volume V , is given by the sum over all the normal modes

$$C = V^{-1} \sum_{\sigma, j} S(\sigma, j). \quad (4)$$

The number of normal modes per unit volume of σ space for a particular polarization j is equal to the crystal volume³⁹ V . The total number of modes in the crystal is

$$\begin{aligned} N_{\text{tot}} &= \sum_i \int_{\sigma} V d\sigma \\ &= \left[V \int_0^\pi d\phi \right] \sum_i \int_0^\pi \left[\sin\theta d\theta \int_0^{\sigma_{\text{max}}} \sigma^2 d\sigma \right], \end{aligned} \quad (5)$$

and is equal to $3\mathfrak{N}$, where \mathfrak{N} is the number of atoms in the crystal. In order to compute C we can now integrate over σ space and sum over the three polarizations:

$$C = \left[\int_0^{2\pi} d\phi \right] \sum_i \int_0^\pi \left[\sin\theta d\theta \int_0^{\sigma_{\text{max}}} S(\sigma, j) \sigma^2 d\sigma \right]. \quad (6)$$

In the low-temperature region the phase and group velocities are equal, and $v_1\sigma_1 = \nu_{10}$. It is assumed that T is sufficiently low so that $h\nu_{\text{max}} \gg kT$ for all directions of σ and polarizations j . Then³⁹

$$C = 9k \left(\frac{\mathfrak{N}}{V} \right) \left(\frac{T}{\theta_0} \right)^3 \int_0^\infty \frac{x^4 e^x dx}{(e^x - 1)^2}, \quad (7)$$

where

$$\frac{1}{\theta_0^3} = \frac{2\pi k^3 V}{9h^3 \mathfrak{N}} \sum_i \left[\int_0^\pi \frac{\sin\theta d\theta}{[v_j(\theta)]^3} \right]. \quad (8)$$

ELASTIC CONSTANTS

Since the v_j values depend on the elastic constants c_{ij} , it is now necessary to substitute numerical values for c_{ij} . There are several published^{32,33,35} estimates of the c_{ij} values for graphite. See Table II for some examples. In the present development, values approximating those of Komatsu^{32,33} are used for c_{11} , c_{12} , and c_{33} . The value for c_{44} is calculated from the experimental

³⁹ M. Born and K. Huang, *Dynamical Theory of Crystal Lattices* (Oxford University Press, Oxford, 1954), p. 63.

TABLE II. The elastic constants of graphite.

Elastic constant	Value in 10^{10} dyn/cm ²			c_{ij}/c_{44} Slack
	Slack	Komatsu ^a	Bowman and Krumhansl ^b	
c_{11}	1000	1000	1130	200
c_{12}	333	312	282	(200/3)
c_{66}^c	333	344	424	(200/3)
c_{13}	~(100)	0	?	0 ^d
c_{33}	33.3	34.9	≥18	(20/3)
c_{44}	5.00	4.05 ^e	2.3	1

^a See reference 33.^b See reference 35.^c $c_{66} = \frac{1}{2}(c_{11} - c_{12})$.^d See text.^e For Canadian natural graphite.

value of the Debye temperature θ_0 in the limit as $T \rightarrow 0^\circ\text{K}$.

The constant c_{13} does not appear in Eq. (2) for the v_j values. Bowman and Krumhansl³⁵ show how c_{13} enters the calculation of the v_j , but they give no estimate for c_{13} . Baker *et al.*⁴⁰ estimate c_{13} as $c_{13} \sim 8 \times 10^{11}$ dyn/cm². If the velocity branches were calculated exactly with the use of nonzero values for c_{13} and c_{44} , then the crossover of $v_2(\theta)$ and $v_3(\theta)$ at $\theta = 9^\circ 35'$ in Fig. 2 would be eliminated. The resultant two branches would be a "high-velocity branch" with velocities 3.83×10^5 cm/sec at $\theta = 0^\circ$ and 21.0×10^5 cm/sec at $\theta = 90^\circ$, and a "low-velocity branch" with a velocity of 1.48×10^5 cm/sec at both $\theta = 0^\circ$ and 90° . The v_1 branch would not be affected. These two new branches would not cross in Fig. 2. They would have velocities at $\theta = 9^\circ 35'$, respectively, of 1.24 times and 0.69 times the present common velocity of 3.79×10^5 cm/sec of v_2 and v_3 . This splitting, indicated by the dashed lines in Fig. 2, would have some effect on the heat capacity and thermal conductivity. However this splitting has been entirely neglected in the present calculation since it is felt that the estimate⁴⁰ of c_{13} is unreliable, and perhaps too high. From here on, it is assumed that $c_{13} = 0$. The nonzero value of c_{44} by itself causes a very small splitting of about 3% in the velocities at the $9^\circ 35'$ crossover. This, too, is neglected.

A calculation of the integral in Eq. (8) can be made in closed form by using Eq. (2). The result is

$$\theta_0 = \frac{h}{k} \left[\frac{3\mathfrak{N}}{4\pi V} \right]^{\frac{1}{3}} \left[\frac{c_{44}}{\rho} \right]^{\frac{1}{3}} \left[\frac{1}{3}(r_1^{-2} + r_2^{-2} + r_3^{-1}) \right]^{-\frac{1}{3}}, \quad (9)$$

where $r_1 = (c_{66}/c_{44})^{\frac{1}{2}}$, $r_2 = (c_{11}/c_{44})^{\frac{1}{2}}$, $r_3 = (c_{33}/c_{44})^{\frac{1}{2}}$. The r_1^{-2} , r_2^{-2} , and r_3^{-1} are the contributions to θ_0 from the frequency branches ν_{10} , ν_{20} , and ν_{30} , respectively. Equation (9), together with Table II, shows that θ_0 is determined mainly by c_{44} and c_{33} , which enter θ_0 from ν_{30} . From Eq. (9) it is evident that the ratios (c_{ij}/c_{44}) are important in determining θ_0 . These same ratios enter again in the computation of K . Thus the calculations are much simplified by convenient nu-

merical values for (c_{ij}/c_{44}). For this reason the numerical ratios given in the fifth column of Table II were used in all of the computations in the present paper. These ratios agree with the values in the second column of Table II, except for c_{13} .

The best experimental value⁴¹ for θ_0 is $420^\circ\text{K} \pm 10^\circ\text{K}$. The value of c_{44} determined from this value of θ_0 , from the absolute values of the other c_{ij} given in the second column of Table II, and from Eq. (9) is $c_{44} = 5.11 \times 10^{10}$ dyn/cm². A value of $c_{44} = 5.00 \times 10^{10}$ dyn/cm² (see Table II) is used throughout the present calculations. This value of c_{44} corresponds to $\theta_0 = 417^\circ\text{K}$, and consequently is quite accurate enough for the present purposes.

THERMAL CONDUCTIVITY

The computation of the two principal thermal conductivities K_{\perp} and K_{\parallel} is similar to that just employed for θ_0 and, hence, C . Let \mathbf{Q} be the net heat flow per unit area per unit time across a plane, where \mathbf{s} is a unit vector normal to this plane. In the relaxation time approximation in which $\tau(\sigma, j)$ is the relaxation time for the phonon mode (σ, j) , the value of \mathbf{Q} is given by

$$\mathbf{Q} = (\mathbf{s}/V) \sum_{\sigma, j} (\mathbf{v}_j \cdot \nabla T) (\mathbf{v}_j \cdot \mathbf{s}) \tau(\sigma, j) S(\sigma, j).$$

Note the summation over all of the modes. Choose a principal direction in the crystal along one of the axes of the thermal conductivity ellipsoid. In graphite these are the a , b , and c axes. The K along the a axis is the same as that along the b axis. For a principal axis \mathbf{s} lies along this axis and is parallel to ∇T . The principal thermal conductivity K_p in the direction \mathbf{s} is

$$K_p = \sum_i \int_{\sigma} (\mathbf{v}_j \cdot \mathbf{s})^2 \tau(\sigma, j) S(\sigma, j) d\sigma. \quad (11)$$

In the pyrolytic graphite sample which was measured, the phonon mean free path l is determined by boundary scattering at the crystallite interfaces over the whole temperature range below about 100°K . Thus

$$\tau(\sigma, j) = l/v_j$$

for all values of σ and j . For the present it is assumed that l is independent of θ and ϕ . For K_{\parallel} , i.e., along the c axis, $\mathbf{v}_j \cdot \mathbf{s} = v_j \cos\theta$. Similarly for K_{\perp} one has $\mathbf{v}_j \cdot \mathbf{s} = v_j \sin\theta \cos\phi$. The anisotropy of the thermal conductivity enters right here in the term $\mathbf{v}_j \cdot \mathbf{s}$. The expression for K_{\parallel} in the limit of low temperatures is now

$$K_{\parallel} = \left[l k \left(\frac{kT}{h} \right)^3 \int_0^\infty \frac{x^4 e^x dx}{(e^x - 1)^2} \right] \left[\int_0^{2\pi} d\phi \right] \times \left[\sum_i \int_0^\pi \frac{\cos^2\theta \sin\theta d\theta}{[v_j(\theta)]^2} \right], \quad (12a)$$

⁴⁰ C. Baker, Y. T. Chou, A. Kelley, *Phil. Mag.* **6**, 1305 (1961).⁴¹ P. Flubacher, A. J. Leadbetter, and J. A. Morrison, *J. Phys. Chem. Solids* **13**, 160 (1960).

while for K_1 we have

$$K_1 = \left[l k \left(\frac{kT}{h} \right)^3 \int_0^\infty \frac{x^4 e^x dx}{(e^x - 1)^2} \right] \left[\int_0^{2\pi} \cos^2 \phi d\phi \right] \times \left[\sum_i \int_0^\pi \frac{\sin^3 \theta d\theta}{[v_j(\theta)]^2} \right]. \quad (12b)$$

By using Eqs. (7) and (8) for the heat capacity per unit volume C , the expressions become

$$K_{11} = lC \left[\sum_i \int_0^\pi \frac{\cos^2 \theta \sin \theta d\theta}{[v_j(\theta)]^2} \right] \left[\sum_i \int_0^\pi \frac{\sin \theta d\theta}{[v_j(\theta)]^3} \right]^{-1}, \quad (13a)$$

$$K_1 = \frac{1}{2} lC \left[\sum_i \int_0^\pi \frac{\sin^3 \theta d\theta}{[v_j(\theta)]^2} \right] \left[\sum_i \int_0^\pi \frac{\sin \theta d\theta}{[v_j(\theta)]^3} \right]^{-1}. \quad (13b)$$

If all of the v_j were equal to \bar{v}_0 and independent of θ , both expressions in Eq. (13) would reduce to

$$K_{11} = K_1 = (l\bar{v}_0 C/3). \quad (14)$$

This is the familiar equation for the thermal conductivity of an isotropic solid in the boundary scattering limit where the phonon mean free path is l .

The \bar{v}_0 in Eq. (14) can be obtained from the expression for θ_0 in Eq. (9). Suppose all the v_j in Eq. (8) were equal to a constant value \bar{v}_0 . This \bar{v}_0 would be given by

$$\bar{v}_0 = \theta_0 (k/h) (4\pi V/3\mathcal{N})^{\frac{1}{3}}.$$

Thus

$$\bar{v}_0 = (c_{44}/\rho)^{\frac{1}{3}} \left[\frac{1}{3} (r_1^{-2} + r_2^{-2} + r_3^{-2}) \right]^{-\frac{1}{3}}. \quad (15)$$

This yields a calculated value for \bar{v}_0 of 2.89×10^5 cm/sec, which is close to the value of v_3 at $\theta = 45^\circ$, and is somewhat less than the average longitudinal velocity of 4.3×10^5 cm/sec measured on the present sample of pyrolytic graphite. The expressions for K_{11} and K_1 in Eq. (13) can now be written in terms of \bar{v}_0 as

$$K_{11} = \left[\frac{l\bar{v}_0 C}{3} \right] \left[\frac{1}{2} \sum_i \int_0^\pi \left(\frac{\bar{v}_0}{v_j} \right)^2 \sin \theta \cos^2 \theta d\theta \right], \quad (16a)$$

$$K_1 = \left[\frac{l\bar{v}_0 C}{3} \right] \left[\frac{1}{4} \sum_i \int_0^\pi \left(\frac{\bar{v}_0}{v_j} \right)^2 \sin^3 \theta d\theta \right]. \quad (16b)$$

The six integrals in Eq. (16) can also be evaluated exactly if Eq. (2) is used. The mathematics is simple but tedious. The results for K_{11} are

$$K_{11} = \left[\frac{l\bar{v}_0 C}{3} \right] \left[\frac{1}{3} \left(\frac{1}{r_1^2} + \frac{1}{r_2^2} + \frac{1}{r_3^2} \right) \right] \left[\sum_i R_j \right], \quad (17)$$

where

$$R_1 = \frac{1}{r_1^2 - 1} \left[\left(\frac{r_1 \ln[r_1 + (r_1^2 - 1)^{\frac{1}{2}}]}{(r_1^2 - 1)^{\frac{1}{2}}} \right) - 1 \right]$$

and

$$R_3 = \frac{1}{r_3^2 - 1} \left[1 - \left(\frac{\arctan[(r_3^2 - 1)^{\frac{1}{2}}]}{(r_3^2 - 1)^{\frac{1}{2}}} \right) \right].$$

The expression for R_2 in terms of r_2 is identical to that for R_1 in terms of r_1 . The expression for K_1 is similar in nature to that for K_{11} . After substituting the c_{ij}/c_{44} ratios in the fifth column of Table II into Eq. (17), the values of K_{11} and K_1 are

$$K_{11} = [l\bar{v}_0 C/3][0.488], \quad K_1 = [l\bar{v}_0 C/3][0.800]. \quad (18)$$

The calculated anisotropy for $T \leq 1^\circ\text{K}$ is therefore

$$K_{11}/K_1 = (0.800/0.488) = 1.64.$$

The fractional contributions of each of the three vibrational branches ν_{10} , ν_{20} , ν_{30} can be computed for K_{11} from the ratios $(R_j/\sum_j R_j)$, etc. These ratios for $j=1, 2, 3$ are, respectively, 21.4%, 9.2%, 69.4%. For K_1 the similar ratios are 3.4%, 1.2%, 95.4%. In both cases the ν_{30} branch, corresponding to the "out-of-plane" vibrations, $j=3$, produces the dominant contribution.

The anisotropy of 1.64, calculated under the assumption that l is constant and independent of θ , is smaller than the experimental value of 2.5. It is known from x-ray studies of the pyrolytic graphite that the crystallites are about twice as large in diameter in the a - b plane as they are thick in the c direction; i.e., $d_1 = 2d_{11}$. Even though the simple analysis showed that l_1 is not equal to d_1 , it is still assumed that $(l_1/l_{11}) = (d_1/d_{11})$. In such a case $l(\theta) = \bar{l}(2)^{\frac{1}{3}}(1 + 3\cos^2\theta)^{-\frac{1}{3}}$, i.e., it is assumed that the crystallites are oblate ellipsoids. The \bar{l} is the diameter of a sphere of the same volume as the mean-free-path ellipsoid. Since $l_1/l_{11} = 2$, $\bar{l} = l_1(2)^{-\frac{1}{3}}$. It turns out that if one takes for $l(\theta)$ the simpler expression

$$l(\theta) = \bar{l}(2)^{\frac{1}{3}}(1 + \cos^2\theta)^{-1}, \quad (19)$$

then the integrals in Eq. (11), where τ is now a function of θ , can be evaluated in closed form. The two different expressions for $l(\theta)$ given above are identical for $\theta = 0^\circ, 90^\circ$. The maximum difference between them is only 6% for any value of θ . Thus the $(1 + \cos^2\theta)^{-1}$ equation for $l(\theta)$ is used. With the ellipsoidal crystallites of graphite:

$$K_{11} = [l\bar{v}_0 C/3][0.403], \quad K_1 = [l\bar{v}_0 C/3][0.913]. \quad (20)$$

The fractional contributions of the ν_{10} , ν_{20} , ν_{30} branches are about the same as before. The calculated anisotropy ratio now is 2.27, which compares favorably with the value of 2.5 measured at 3°K , the lowest temperature reached. The anisotropy as a function of temperature should asymptotically approach the value of 2.27 as T approaches 0°K . The experimental ratio of K_1/K_{11} for the present sample of pyrolytic graphite (PG-0) in Fig. 3 appears to be approaching a limiting value of 2.2 to 2.4 for $T \leq 1^\circ\text{K}$.

The calculated value of the anisotropy is determined mostly by the ν_{30} branch, and hence by r_3 . In order to show the effect of a change³⁵ in c_{44} on the calculated anisotropy, c_{44} was both increased and decreased by a factor of 2. All the other c_{ij} were held constant. The

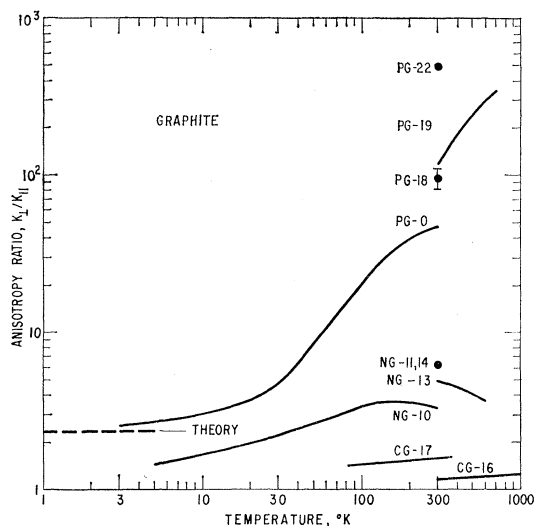


FIG. 3. The measured values of the anisotropy in the thermal conductivity, K_1/K_{11} , as a function of temperature for samples of pyrolytic (PG), natural (NG), and commercial (CG) graphite. For PG-0 the theory predicts a limiting value of 2.27 for $T \leq 1^\circ\text{K}$. This is indicated by the dashed line.

results for the ellipsoidal crystallites are

$$\begin{aligned} c_{44} &= 10.0 \times 10^{10} \text{ dyn/cm}^2, & K_1/K_{11} &= 1.71; \\ c_{44} &= 5.0 \times 10^{10} \text{ dyn/cm}^2, & K_1/K_{11} &= 2.27; \\ c_{44} &= 2.5 \times 10^{10} \text{ dyn/cm}^2, & K_1/K_{11} &= 3.06. \end{aligned} \quad (21)$$

As c_{44} increases toward c_{11} , c_{12} , etc., the anisotropy decreases. For spherical particles the K_1/K_{11} values in Eq. (21) should be reduced by 1.38 ± 0.01 for all three cases. The $5.00 \times 10^{10} \text{ dyn/cm}^2$ for c_{44} derived from θ_0 gives a better fit to the measured anisotropy in K than do either of the other values of c_{44} .

Several other features of the calculated anisotropy should be mentioned. First, the (l_1/l_{11}) ratio of 2 rather than 1 produces an increase in the calculated anisotropy by a factor of only 1.38 instead of 2.00. This reduction in the effect of the crystallite shape is caused by the weighted averaging of $l(\theta)$ over the interval $0^\circ \leq \theta \leq 90^\circ$. Equations (20) and (21) give an anisotropy value in good agreement with the observed value. The effect of allowing l but not v_j to be anisotropic can also be evaluated from Eq. (11). This is done by setting all the v_j equal to \bar{v}_0 and making τ a function of θ . If Eq. (19) for $l(\theta)$ is used, then

$$K_{11} = [\frac{1}{3} \bar{l} \bar{v}_0 C] [0.811], \quad K_1 = [\frac{1}{3} \bar{l} \bar{v}_0 C] [1.079]. \quad (22)$$

Thus the anisotropy K_1/K_{11} produced by the crystallite shape alone is 1.33. The anisotropy produced by the elastic constants alone is 1.64. The two effects are of comparable importance in determining K_1/K_{11} . The product $1.33 \times 1.64 = 2.18$ is somewhat less than the anisotropy of 2.27, which is produced by both effects operating simultaneously.

Next, consider the absolute value of \bar{l} . At 1°K the extrapolated value of K is $1 \times 10^{-5} \text{ W/cm deg}$. With a lattice heat capacity determined from θ_0 at 1°K of $C = 4.95 \times 10^{-6} \text{ J cm}^3 \text{ deg}$, the experimental phonon mean free path is $\bar{l} = 2000 \text{ \AA}$. This is 10 times larger than the average diameter of the crystallites $\bar{d} = 220 \text{ \AA}$, as determined by the x-ray line broadening. Since \bar{l} and \bar{d} are really determined by much different techniques, it is not surprising that they are unequal. It can be conjectured that the crystallite "boundaries" are not terribly effective in scattering phonons. Perhaps the long-wavelength phonons travel through about 10 crystallites before being scattered. The anisotropy in K for $T \leq 1^\circ\text{K}$ is not influenced by the absolute value of l_1 or l_{11} , providing l_1 and l_{11} are much less than the diameter ($\sim 0.5 \text{ cm}$) of the sample. The K_1/K_{11} value depends on the ratio l_1/l_{11} . Similarly K_1/K_{11} depends on the ratios c_{ij}/c_{44} , but not on the absolute magnitude of the c_{ij} . This means that the anisotropy in K can be calculated with a higher precision than the absolute value K .

ANISOTROPY FOR $T \gg 1^\circ\text{K}$

None of the considerations used so far, in which the graphite crystallites are treated as an elastic continuum yield an anisotropy in K of the order of 100. By contrast, the experimental values of K_1/K_{11} at 300°K for pyrolytic graphite vary from 50 to 500. The marked increase in K_1/K_{11} as T increases toward 300°K , shown in Fig. 3, requires a different explanation. This marked increase is probably caused by the gradual excitation of the plane-bending vibrations considered by Komatsu and Nagamiya³¹⁻³³ and by the low heat capacity, low effective temperature, and low velocity of the modes primarily associated with c_{44} and c_{33} .

For a very crude analysis at temperatures between 10° and 100°K let us consider only the v_{30} vibrational branch. It has just been shown that this branch is responsible for most of the thermal conductivity for $T \leq 1^\circ\text{K}$. It is also responsible³² for most of the heat capacity up to 90°K . The group velocity³² for a mode of this branch at $\theta = 90^\circ$ (i.e., in the graphite planes) is approximately $v_3(90^\circ) \sim 4\pi\kappa\sigma_x$, while for $\theta = 0^\circ$ one obtains $v_3(0^\circ) \sim (c_{33}/\rho)^{1/2} \cos(\pi c\sigma_x)$. At, say, 100°K one can estimate $\sigma_x \sim \lambda_x^{-1} \sim T/(a_0\theta_x)$, where θ_x is an effective Debye temperature of, maybe, 1000°K , and a_0 is the lattice constant in the x - y plane. For λ_x the wavelength of the most numerous phonons at 100°K has been used, i.e., approximately $(a_0\theta_x/T)$. At 100°K $\sigma_x \sim (2c)^{-1}$, which makes $v_3(0^\circ) \sim 0$. As T approaches 0°K , then $v_3(0^\circ)$ approaches $(c_{33}/\rho)^{1/2}$. A weighted $v_3(0^\circ)$ at 100°K might be $\sim \frac{1}{5}(c_{33}/\rho)^{1/2}$. The anisotropy in K computed just from v_3 is, crudely,

$$\frac{K_1}{K_{11}} \sim \frac{v_3(90^\circ)}{v_3(0^\circ)} \sim \left[\frac{20\pi\kappa}{a_0\theta_x} \left(\frac{\rho}{c_{33}} \right)^{1/2} \right] T. \quad (23)$$

This ratio is essentially the ratio of the velocity of the bond-bending, in-plane vibration to the velocity of the compressional, out-of-plane vibration. The anisotropy increases nearly linearly with increasing temperature, as the experimental results in Fig. 3 show for PG-0. If the values given by Komatsu are used, i.e., $\kappa = 6.11 \times 10^{-3}$ cm²/sec, $a_0 = 1.415 \times 10^{-8}$ cm, $(c_{33}/\rho)^{1/2} = 3.92 \times 10^5$ cm/sec, then $K_{\perp}/K_{\parallel} \sim 7$ at 100°K. The measured anisotropy at 100°K is 20 for PG-0 in Fig. 3. The temperature T_c at which the anisotropy in K changes from that given by Eqs. (18) and (20) to that given by Eq. (23) is, according to Komatsu,³²

$$T_c = (hc_{44}/4\pi\rho k k).$$

Komatsu³² gives 2.13°K for T_c . However, the present value of c_{44} of 5.00×10^{10} dyn/cm² is 6.7 times greater than his. Hence, $T_c = 14^\circ\text{K}$ in the present calculations. The simple elastic theory is, therefore, good for $T \leq 0.1T_c = 1.4^\circ\text{K}$. The upper limit of 1°K , used throughout the present calculations, appears adequate. A T_c of 14°K agrees with Fig. 3 where the transition from a temperature independent K_{\perp}/K_{\parallel} to a $K_{\perp}/K_{\parallel} \sim T$ occurs between 10° and 20°K . It should not, however, be assumed that Eq. (23) is at all accurate. A rigorous calculation of K_{\perp}/K_{\parallel} vs T for $T > T_c$ would be more complicated than the calculation of the heat capacity.^{33,39} Such a calculation of K has not yet been made.

SOME SPECULATIONS

The anisotropy in K as a function of T is plotted in Fig. 3 for a number of samples. The results for specimens of natural graphite (NG) and commercial graphite (CG) all show anisotropy ratios $K_{\perp}/K_{\parallel} \leq 6$. Furthermore the measured anisotropy varies only slowly with temperature. The results on the pyrolytic graphite (PG) samples all indicate that $K_{\perp}/K_{\parallel} \geq 50$ at and above 300°K . It is concluded that the results for the PG samples are more nearly representative of single crystal graphite. All of the present theoretical calculations have been made for an idealized single crystallite of graphite.

The data in Fig. 1 suggest that at 300°K the K_{\parallel}

value of about 2×10^{-2} W/cm deg is determined by phonon-phonon interactions while K_{\perp} for the samples PG-0, 18, 20, 21 is still limited by the crystallite size. Perhaps the K_{\perp} value for PG-24 at 300°K of 29 W/cm deg is determined by phonon-phonon interactions. Therefore, pyrolytic graphite with a crystallite size of $> 10^{-3}$ cm might exhibit a $K_{\perp}/K_{\parallel} \simeq 10^3$ at 300°K . This estimated limiting value is included in Table I for comparison with the experimental results. The anisotropy in the electrical conductivity of single crystal graphite at 300°K is even larger than that in K . It is estimated⁴² that for single crystals of graphite $\sigma_{\perp}/\sigma_{\parallel} \simeq 2 \times 10^4$.

CONCLUSIONS

The anisotropy in the thermal conductivity K of pyrolytic graphite for temperatures $\leq 1^\circ\text{K}$ lies between 2 and 3. Its exact value is determined by the elastic constants c_{ij} , and by the ellipsoidal shape of the crystallites. For higher temperatures the bond-bending vibrations of the loosely coupled graphite sheets appear to be responsible for the rapid rise in K_{\perp}/K_{\parallel} for $T > 14^\circ\text{K}$. It is suggested that in well-oriented graphite samples with a crystallite size greater than $\sim 10^{-3}$ cm, the anisotropy in K might be as large as 10^3 at 300°K .

Note added in proof. Some more extensive measurements on the thermal conductivity of pyrolytic graphite have recently been made. These confirm the general results shown in Figs. 1 and 3. [See M. G. Holland and C. A. Klein, Bull. Am. Phys. Soc. 7, 191 (1962).]

ACKNOWLEDGMENTS

The author would like to thank R. J. Diefendorf and E. R. Stover for the samples of pyrolytic graphite, and for illuminating discussions concerning the nature of pyrolytic graphite. Thanks are extended to J. H. McTaggart for his able assistance in measuring the thermal conductivity, and to B. W. Roberts for his measurements of the sound velocity. Conversations with B. T. Bernstein, G. Dolling, M. G. Holland, and R. E. Jones on graphite are also acknowledged.

⁴² R. J. Diefendorf (private communication).